Int. J. Electrochem. Sci., 16 **(2021)** Article Number: 211232, doi: 10.20964/2021.12.27

International Journal of
ELECTROCHEMICAL
SCIENCE
www.electrochemsci.org

Short Communication

Synthesis and Application of Ag NPs@graphene Oxide Nanocomposite as an Electrochemical Sensor for Sweat Lactate Monitoring in Sports Medicine

Wenhong Wang

Department of Physical Education, Jinling Institute of Technology, Nanjing, 211169, China
E-mail: wwh@jit.edu.cn

Received: 28 August 2021 / *Accepted:* 9 October 2021 / *Published:* 10 November 2021

In this study, a sensitive electrochemical sensor for detection of lactate was proposed. The sensor was developed based on GCE substrate coated by Ag NPs@GO/GCE. The morphological and structural properties of Ag NPs@GO/GCE were characterized using FESEM and XRD analysis, respectively. FESEM results confirmed a uniform distributed Ag NPs in GO nanocomposites. The sensor performance of the device was examined by amperometry and cyclic voltammetry. The electrochemical sensor exhibited a linear response to the lactate in phosphate buffer solution with a liner range and sensitivity of 10 to 600 µM and 16.5 μAcm^{-2} mM^{-1}, respectively. The concentration of lactate estimated by this sensor in real sweat samples was very close to the amount of injection which can be considered as a sensor for lactate measurement in sweat samples.

Keywords: Electrochemical sensor; lactate; Ag NPs@graphene oxide nancomposites; Cyclic voltammetry

1. INTRODUCTION

The clinical diagnosis of a commonly assessed significant parameter, lactate concentration, is used in the assessment of a person's health form, pathology, and regular health inspection in surgery, sports medicine, severe mental/physical pain, and food industries [1]. The level can go up to 25 mmol/L based on the intensity of the activity [2]. Besides being generally used in health management the food industry, lactate tracking plays a vital role in conditions like respiratory failure, tissue hypoxia, hemorrhage, sepsis, and liver disease [3, 4]. The traditional methods used to determine lactate levels are inaccurate and slow and hence there is a demand for a sensor with high sensitivity and high input screening of lactate in various samples [5]. So, excessive consideration has been pinched to evolving low-cost transportable devices, particularly electrochemical sensors, for fast, real-time monitoring of the lactate level.

The surface modification of graphene oxide (GO) has opened up a plethora of possibilities for its use in the development of nanocomposite materials [6]. The GO has a high conductivity and can be used in a variety of fields, including electronics, anticancer properties, sensors, photocatalytic activity, antibacterial coatings in biomedicine, drug delivery, solar desalination, and water decontamination [7].

In specific, 1-dimensional nanostructures have been found to be up and coming for use in sensors, optics, actuators, and optoelectronics due to the 1-dimensional structures that enable them to possess inviting, not limited to, piezoelectric, semiconducting, and pyroelectric properties as mentioned in previous studies [8, 9]. Because of their electro-catalytic efficacy, high aspect ratios, and quick electron communication, they are suitable for enhanced immobilization and the required transducing phenomena. Ag is the most reactive and conductive of the transition elements, and it has recently been used to make Ag-doped GO with promising features such as increased mechanical strength, superior dispersion, and low resistance [10]. Ag nanoparticles have recently gained popularity in sensor applications due to their antibacterial properties [11]. Yet, increasing the efficacy of sensors is to be achieved. In the current work, Ag NPs@graphene oxide composites were effectively grown on glass carbon electrodes (GCE) using a facile method that combines an electrochemical process with an aqueous solution method. Furthermore, physical and electrochemical results of lactate detection using Ag NPs@GO/GCE bioelectrode with nano-interface have been reported.

2. MATERIALS AND METHOD

GO was synthesized using a modified Hummers procedure in which graphite was reacted with concentrated H_2SO_4 after being treated with $NaNO_3$ and $KMnO_4$ [12]. 1.2 g of graphite powder and 2g of sodium nitrate were put in a beaker containing 50mL of determined H_2SO_4. After stirring the reaction mix in ice-cold water for one hour while maintaining a temperature of 0-5°C, 6g of $KMnO_4$ was gradually added to the reaction mix. The specimen mix was agitated continuously for one hour at 40°C until it turned into a brownish paste, then stirred continuously for another one hour for each half-hour rise in temperature. The solution mix was finally treated with 8mL of H_2O_2 to terminate the reaction. The addition of H2O2 resulted in a rapid change in color from dark brown to golden yellow, indicating the formation of GO. The mixture was then washed and centrifuged several times with 8% HCl before being rinsed with deionized (DI) water. The precipitates that formed were dried, filtered, and finely powdered.

Solution-A of silver nitrate ($AgNO_3$) was prepared for the production of Ag NPs by dissolving 3.4g of silver nitrate in 20mL DI water. 1g of PVP, 1g glucose, and 1g NaOH were combined in 60mL of DI water to make Solution-B of polyvinylpyrrolidone (PVP). Solution-B was heated to 70°C by continuous stirring before adding solution-A dropwise. The finished product was then mixed for 20 minutes. To extract Ag NPs, the mixture was rinsed, centrifuged, and dried with DI water.

The Ag NPs@GO nanocomposite was produced by mixing Ag and GO in a 1:2 ratio in 50mL of methanol. The mix was sonicated for two days before being thermally annealed at 400°C and then cold frozen at -20°C; the entire procedure was repeated two times. Finally, the powder obtained was homogenized and dried.

Electrochemical studies were performed with an Eco-Chemie Autolab PGSTAT12 system using a cell with tri compartments, a working Ag NPs@GO/GCE electrode along with a platinum wire in place of the counter electrode. The potentials of the Ag/AgCl reference electrode were observed and noted. The Lactate solution was made by mixing 5.0 mg Lactate in 1.0mL of phosphate-buffered saline (PBS) solution. 20 µL of the solution was let fall onto the surface of electrodes and permitted to dry in ambient conditions. The Ag NPs@GO/GCE electrode was characterized by a field-emission scanning electron microscope (FE-SEM, SUPRA-55, Zeiss). The structural characteristics of the Ag NPs@GO nanocomposite were studied using an X-ray Diffractometer (XRD) (D8 Focus, Bruker, Germany). Cyclic voltammetry (CV) experiments were carried out by cycling the working electrode between -0.1 to -0.4 V at a scan rate of 10mV/s. The charge transfer process was also examined by EIS in the frequency range from 0.1 Hz to 10^5 Hz at an AC voltage of 10mV amplitude. The electrolyte for the EIS measurement was 0.1 M KCl (99%) solution containing 5mM $[Fe(CN)_6]^{3-/4-}$ (99.5%). Real samples were taken from the sweat of several athletes and examined instantly following their response. A small portion of 950 µL whole sample was mixed with 50 µL of lactate solution (0.1M) to make a recovering analysis of the sensor.

3. RESULTS AND DISCUSSION

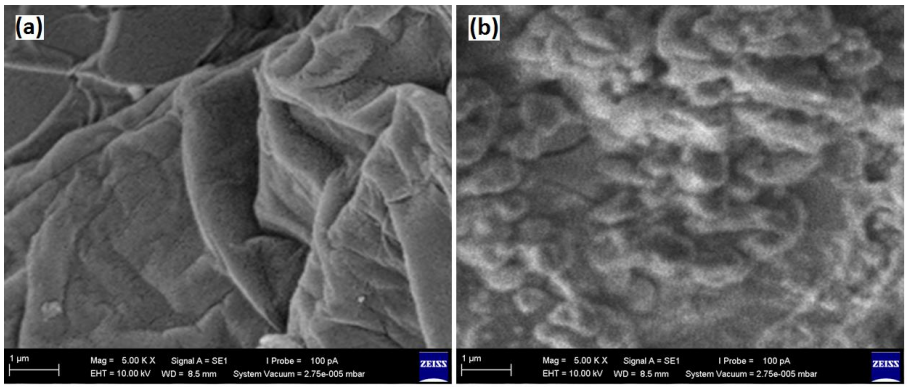

Figure 1. FESEM images of (a) prepared GO/GCE and (b) Ag NPs@GO/GCE.

The morphology of GO/GCE and Ag NPs@GO/GCE are shown in FESEM images from Fig. 1. The GO/GCE are arranged into wrinkled formations that resemble crumpled silk veils, as seen. As the nanosheets were oriented at different angles, they rippled and became entangled with one another. Ag NPs@GO/GCE are integrated in GO nanostructure in a spherical form including an average diameter of 150 nm, as seen in the FESEM image. Because of repulsion interactions between the irregularly agglomerated nanostructures on the GO surface, the GO nanostructure is robustly and irregularly adorned with Ag NPs.

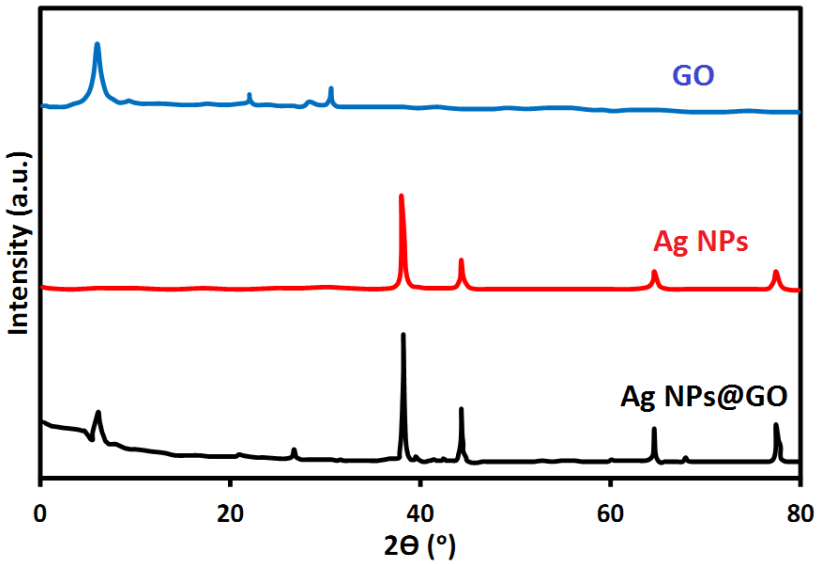

Figure 2. XRD patterns of GO, Ag NPs and Ag NPs@GO nanocomposites.

The XRD patterns of prepared GO, Ag NPs, and Ag NPs@GO nanocomposites is shown in Figure 2. GO's XRD pattern shows a strong 2θ=10.18° values that corresponds to a (001) plane. Moreover, a minor peak at 2θ=20.87° was obtained, which reveals the (002) plane. The interlayer space in GO structures improved when compared to graphite due to the oxygen-containing functional groups created by graphite oxidation [13]. Ag NPs revealed a major diffraction peak at 2θ =38.149° representing the plane of (111) and corresponding to the previous reported literature [14]. The Ag NPs@GO nanocomposite indicated a peak associated to both Ag NPs and GO. However, as shown in Fig.2, a slight shift in peak position to lower 2θ values indicates intercalation of Ag NPs in GO nanoconposite.

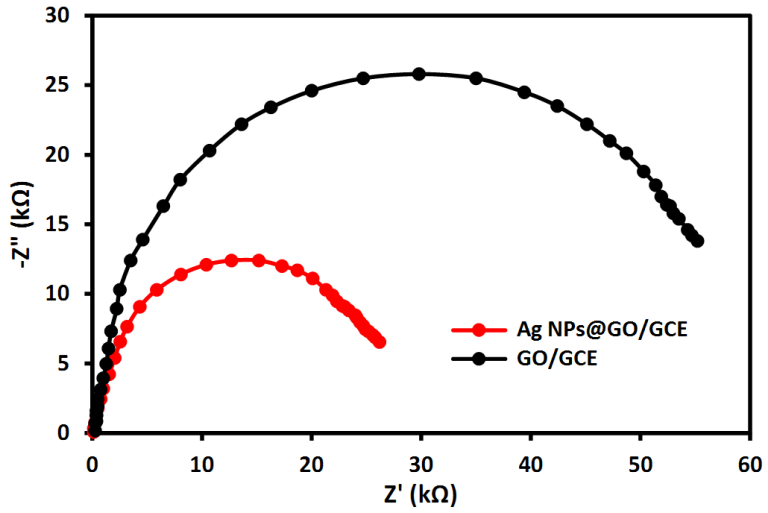

Figure 3. EIS Nyquist plots of GO and Ag NPs@GO nanocomposites in 0.1 M KCl containing 5mM $[Fe(CN)_6]^{3-/4-}$ redox probe solution with frequency range of 0.1 Hz to 10^5 Hz at AC voltage of 10 mV amplitude..

EIS is a well-known and powerful device for determining charge separation and transfer in sensor applications [15]. EIS was used to further clarify the effect of Ag NPs on the charge separation process in GO nanocomposites. The electron transfer resistance at the electrode surface is indicated by the arc radius seen in the EIS spectra. It can be seen in figure 3 that the arc radius of Ag NPs@GO/GCE is less than the arc radius seen for GO/GCE suggesting that the former has better parting of charges and quick interfacial transferring of charges than the latter. The EIS results show that the use of Ag NPs in the GO structures can efficiently advance charge transfer. This provides a new and improved alternative material for the fabrication of sensors.

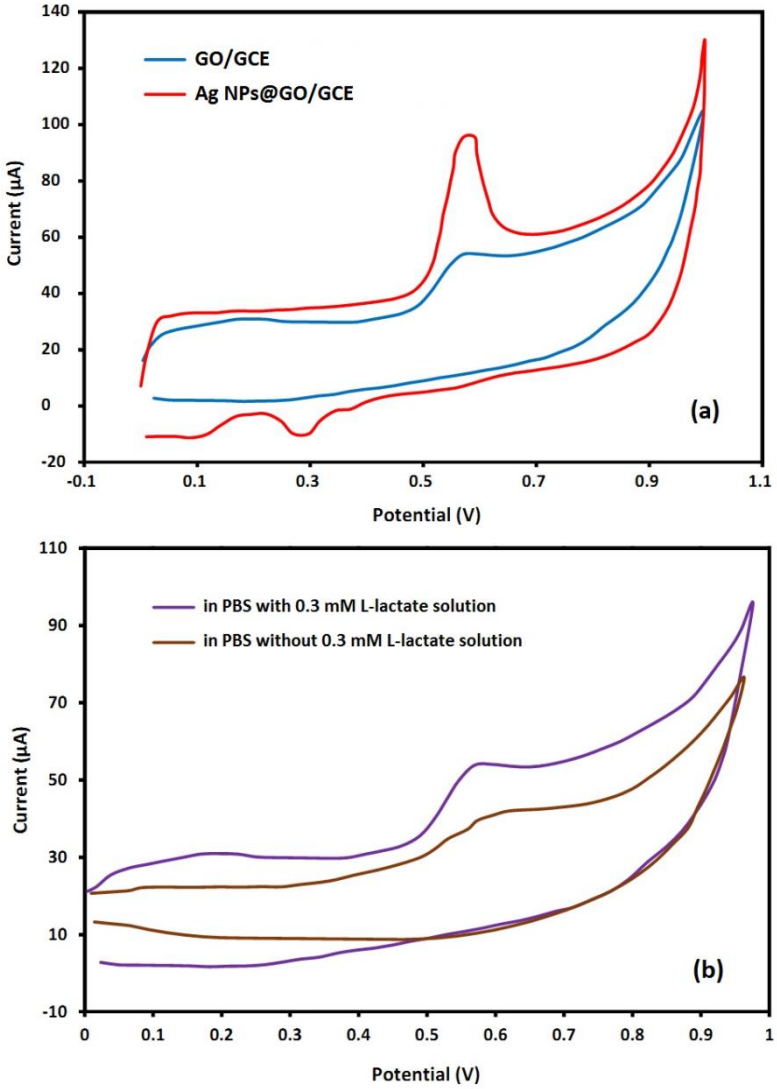

Figure 4. CV plots of (a) the GO/GCE and Ag NPs@GO/GCE electrodes at a 50 mV s^{-1} scan rate, (b) the Ag NPs@GO/GCE electrode in 0.3 mM lactate solution

The impact of Ag NPs@GO/GCE electrode on the membrane's electrical conductance was assessed by CV. The efficiency of the GO/GCE and Ag NPs@GO/GCE electrodes in the PBS (pH 7.0) is almost equal, as seen in Figure 4a. According to them, the Ag NPs@GO/GCE electrode has improved the current response of the lactate sensor in the PBS solution. Two noticeable peaks at

around 0.59 V and 0.28 V in the CV plot, correspondingly relating to oxidation and reduction are seen. It is obvious from the curve that Ag NPs@GO/GCE have a vital impact on the semipermeable altered electrode. These deliver a high number of conductive paths from the lactate to the electrode and thus develop the electron transfer of Ag NPs@GO/GCE electrode.

Figure 4b demonstrates the change in CV curves among the Ag NPs@GO/GCE electrodes in the PBS in the presence and absence of 0.3 mM lactate. The current surges from 0.26 to 0.57 V in a 0.3 mM lactate solution related to that in the PBS lacking lactate. This is attributed to the catalytic reaction of the electrode with lactate. An apparent peak is seen at around 0.57 V on the CV plot for the Ag NPs@GO/GCE electrode in 0.3 mM lactate with 0.1M PBS. This peak may be ascribed to hydrogen peroxide produced while the catalysis of lactate oxidation occurs. Electrons produced from the reduction-oxidation reaction of hydrogen peroxide over the electrode have played a vital role in improving the current response [16].

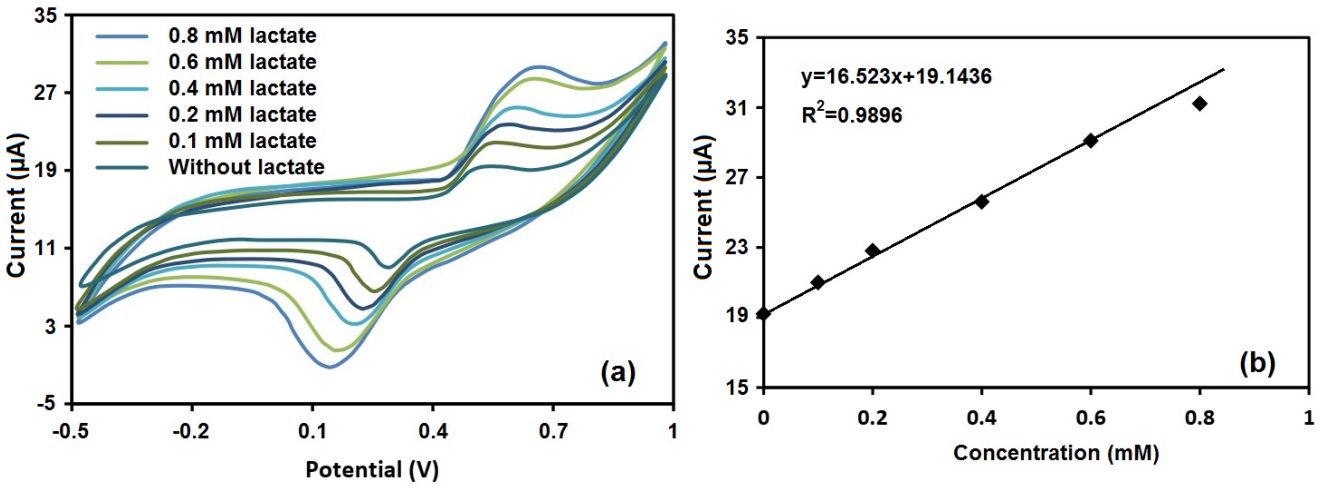

Figure 5. (a) CV response for Ag NPs@GO/GCE sensor in interaction with a 0.1 M PBS (pH 7.0) without and with 0.1 to 0.8 mM of lactate (b) Calibration curve plotted from the mentioned CV responses.

To the best of our knowledge, no electrochemical sensor containing Ag NPs@GO/GCE nanostructures had been developed prior to this work. Because of this, the response is based on the oxidation of lactate to pyruvate, which is catalyzed by lactate. Figure 5a portrays the CV response for the Ag NPs@GO/GCE electrode with and without the cumulative concentrations of lactate in 0.1 M phosphate buffer solution (pH 7.0). The investigative parameters (reproducibility, sensivity, repeatability, linear range of concentration, and limit of detection) are found. Figure 5b illustrates a linear calibration plot from a 10 to 600 µM range of concentration (R^2 = 0.9896). The sensitivity, estimated from the gradient of the plot, was found to be 16.5µAcm^{-2} mM^{-1}.

Table 1. Comparison of Ag NPs@GO/GCE sensor performance with other lactate sensors.

Method	Electrode type	Sensitivity (μAcm^{-2} mM^{-1})	Limit of detection (mM)	Ref.
CV	Ag NPs@GO/GCE	16.5	6.0	This work
Amperometric	FcMe2-LPEI	45	3.0	[17]
Amperometric	Gold	37.1	11.5	[18]
Amperometric	GNWs/LOx/PET	18	1.0	[19]
Amperometric	PtNp-CNF-PDDA/SPCEs	36.8	11.0	[20]
CV	GOx/DNPs/Au	5.0	15.0	[21]
Amperometric	MWCNT/FcMe/CS/HRP/ BSA/LOx/SPBGE	3417	22.6	[22]

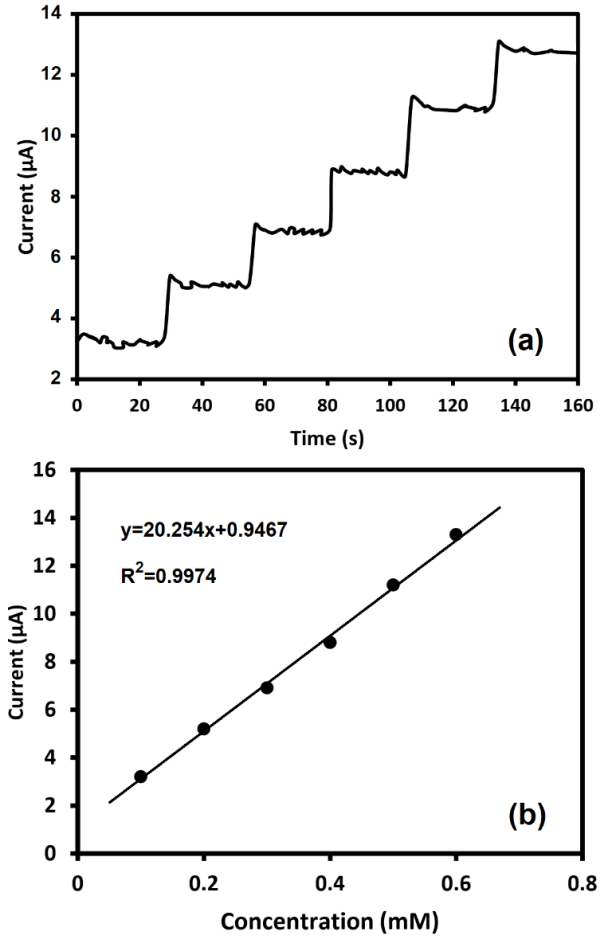

Figure 6. (a) The recorded amperometrogram of Ag NPs@GO/GCE in 0.1 M PBS also of different concentrations of lactate in a real sample; (b) Plot of the calibration curve.

As shown in Table 1, this LOD is comparable to those obtained from other methods used to determine lactate in general, which can be attributed to their higher aspect ratio and longer carrier lifespan than others. The repeatability was assessed by relative standard deviation (RSD) which was calculated by 9 varied readings of a 5 mM lactate concentrate using a constant sensor. A value of RSD

was received as 5%. The storage stability was assessed, deciding it held 50% of its earlier responses 15 days later. From these results, it can be concluded that the usage of Ag NPs@GO nanocomposites to fabricate lactate sensor permits procurement of an analytical response which is analogous to those obtained by other nanomaterials. Furthermore, the sensor developed in this study has advantages such as a simple fabrication process and the use of a low-cost nanomaterial.

Because the sensor is highly stable, it is possible to use it to accurately assess the lactate level in sweat samples. The concentration of lactate in sweat was measured to investigate the Ag NPs@GO/GCE electrode for determining lactate in real samples. The standard injection of lactate was used to determine lactate in the sweat sample. Figure 6a shows the recorded amperometrogram of the Ag NPs@GO/GCE prepared sample of sweet in successive injections of 0.1 mM lactate solution. Figure 6b shows the calibration curve with a correlation coefficient of 0.9974. Therefore, the concentration of lactate was estimated at 0.229 mM in 0.1M PBS and 0.167 mM in pure sweat, which were very close together. The results show that Ag NPs@GO/GCE can be considered as a sensor for lactate measurement in sweat samples.

4. CONCLUSIONS

Sweat lactate concentration is one of the most important parameters measured when testing athletes' performance. In this study, a sensitive electrochemical sensor was fabricated to detect lactate using a facile technique. The sensor was developed based on the GCE substrate coated with Ag NPs@GO/GCE. The morphological and structural properties of Ag NPs@GO/GCE were characterized using FESEM and XRD analysis, respectively. FESEM results confirmed the uniform distribution of Ag NPs in GO nanocomposites. The sensor performance of the device was examined by amperometry and cyclic voltammetry. The electrochemical sensor exhibited a linear response to the lactate in phosphate buffer solution with a liner range and sensitivity of 10 to 600 µM and 16.5 μAcm^{-2} mM^{-1}, respectively. The concentration of lactate estimated by this sensor in real sweat samples was very close to the amount of injection which can be considered as a sensor for lactate measurement in sweat samples.

References

1. K. Rathee, V. Dhull, R. Dhull and S. Singh, *Biochemistry and biophysics reports*, 5 (2016) 35.
2. P. Claus, A.M. Gimenes, J.R. Castro, M.M. Mantovani, K.K. Kanayama, D.M. Simões and D.S. Schwartz, *The Canadian Veterinary Journal*, 58 (2017) 817.
3. W. Zhang, X. Li, Y. He, X. Xu, H. Chen, A. Zhang, Y. Liu, G. Xue and J. Makinia, *Bioresource Technology*, 302 (2020) 122881.
4. Y. Wang, *International Journal of Electrochemical Science*, 15 (2020) 1681.
5. J.M. Colon-Franco, S.F. Lo, S.S. Tarima, D. Gourlay, A.L. Drendel and E.B. Lerner, *Clinica Chimica Acta*, 468 (2017) 145.
6. W. Hou, Y. Gao, J. Wang, D.J. Blackwood and S. Teo, *Materials Today Communications*, 23 (2020) 100883.

7. S. Kumari, P. Sharma, S. Yadav, J. Kumar, A. Vij, P. Rawat, S. Kumar, C. Sinha, J. Bhattacharya and C.M. Srivastava, *ACS omega*, 5 (2020) 5041.
8. C.-L. Hsu, J.-H. Lin, D.-X. Hsu, S.-H. Wang, S.-Y. Lin and T.-J. Hsueh, *Sensors and Actuators B: Chemical*, 238 (2017) 150.
9. B. Tao, R. Miao, W. Wu and F. Miao, *International Journal of Electrochemical Science*, 12 (2017) 7216.
10. N. Mustaffa, M. Rahman and A. Umar, *Ionics*, 24 (2018) 3665.
11. A.A. Yaqoob, K. Umar and M.N.M. Ibrahim, *Applied Nanoscience*, 10 (2020) 1369.
12. D.C. Marcano, D.V. Kosynkin, J.M. Berlin, A. Sinitskii, Z. Sun, A. Slesarev, L.B. Alemany, W. Lu and J.M. Tour, *ACS nano*, 4 (2010) 4806.
13. V. Gupta, N. Sharma, U. Singh, M. Arif and A. Singh, *Optik*, 143 (2017) 115.
14. R. Janardhanan, M. Karuppaiah, N. Hebalkar and T.N. Rao, *Polyhedron*, 28 (2009) 2522.
15. J. Xu, *International Journal of Electrochemical Science*, 12 (2017) 2253.
16. S. Jafari, N. Nasirizadeh and M. Dehghani, *Journal of Electroanalytical Chemistry*, 802 (2017) 139.
17. D.P. Hickey, R.C. Reid, R.D. Milton and S.D. Minteer, *Sensors and bioelectronics*, 77 (2016) 26.
18. L.V. Shkotova, N.Y. Piechniakova, O.L. Kukla and S.V. Dzyadevych, *Food chemistry*, 197 (2016) 972.
19. Q. Chen, T. Sun, X. Song, Q. Ran, C. Yu, J. Yang, H. Feng, L. Yu and D. Wei, *Nanotechnology*, 28 (2017) 315501
20. P.J. Lamas-Ardisana, O.A. Loaiza, L. Añorga, E. Jubete, M. Borghei, V. Ruiz, E. Ochoteco, G. Cabañero and H.J. Grande, *Sensors and bioelectronics*, 56 (2014) 345.
21. M. Briones, E. Casero, M. Petit-Domínguez, M. Ruiz, A. Parra-Alfambra, F. Pariente, E. Lorenzo and L. Vázquez, *Sensors and bioelectronics*, 68 (2015) 521.
22. N. Hernández-Ibáñez, L. García-Cruz, V. Montiel, C.W. Foster, C.E. Banks and J. Iniesta, *Sensors and bioelectronics*, 77 (2016) 1168.